Evaluating Pseudorange Multipath Effects at Stations in the National CORS Network

Stephen Hilla
Michael Cline
National Geodetic Survey, NOS/NOAA
Silver Spring, Maryland 20910

A poster paper presented at the
Weikko A. Heiskanen Symposium in Geodesy
The Ohio State University
Columbus, Ohio
1 – 4 October, 2002

Evaluating Pseudorange Multipath Effects at Stations in the National CORS Network

Stephen Hilla, Michael Cline
National Geodetic Survey, NOS/NOAA
Silver Spring, Maryland 20910

Abstract:
A preliminary study has been conducted to evaluate the amount of pseudorange multipath at 390+ sites in the National Continuously Operating Reference Station (CORS) Network. The National CORS Network is a cooperative effort involving over 60 different agencies, universities, and private companies who seek to make available to the general public GPS data from dual-frequency receivers located throughout the United States and its territories. For CORS users, pseudorange multipath can seriously degrade the accuracy of any application that relies on precise measurements of the pseudorange observable over a short period of time, including differential pseudorange navigation, kinematic and rapid-static surveying, and ionospheric monitoring. The main objectives of this study were to identify the most affected and least affected sites in the network, to closely investigate problematic sites, and to compare various receiver/antenna combinations. Dual-frequency carrier phase and pseudorange measurements were used to estimate the amount of L1 and L2 pseudorange multipath at each site over a one year period. Some of the most severely affected sites were maritime Differential GPS and Nationwide Differential GPS (DGPS/NDGPS) sites. Photographs obtained for these sites verified the presence of transmission towers and other reflectors in close proximity to the GPS antennas. Plotting the variations of the L1 and L2 pseudorange multipath with respect to azimuth and elevation further verified that even above a 60° elevation angle there was still as much as five meters of pseudorange multipath at some sites. The least affected sites were the state networks installed in Ohio and Michigan; these sites used excellent antenna mounts, choke ring antennas, and new receiver technology. A comparison of the 12 most commonly used receiver/antenna combinations in the CORS Network seemed to indicate that newer receivers such as the Ashtech UZ-12, Leica RS-500, and Trimble 5700 help to significantly mitigate pseudorange multipath, while the receivers/antennas at some DGPS/NDGPS sites, and at the Wide Area Augmentation System (WAAS) sites, seem to be among those most affected by pseudorange multipath. The receiver/antenna comparison did not take into account the potential presence of reflectors at the sites (i.e., it is possible that a well-performing receiver/antenna combination could have been placed at very poor site locations, and vice-versa).

1 Introduction

An initial study has been done to estimate the amount of pseudorange multipath at 390+ sites in the National CORS Network. The study was conducted to identify the most affected and least affected sites in the network, to compare different receiver/antenna combinations, and to investigate closely those sites which appear to be severely affected by multipath. Identification of severely affected sites will help with other research at the National Geodetic Survey (NGS), such as ionospheric studies (mapping Total Electron Content), studies related to the High Accuracy National Differential Global Positioning System (HA-NDGPS) demonstration project, and studies done to evaluate different methods for pseudorange multipath calibration (e.g., Bishop et al. 1994, Kee and Parkinson 1994) and carrier phase multipath calibration (e.g., Wanninger and May 2001, Brown and Wang 1999, Ray 1999). Comparing different receiver/antenna combinations will highlight the equipment and the antenna mounting techniques that seem to be working best in the current network. Closely investigating the most severely affected sites, both by examining photographs and by analyzing multipath variations with respect to elevation angle and azimuth, will help lead to a better understanding of the kinds of factors contributing to pseudorange multipath at a site.

Our main tool for calculating the variation of the L1 and L2 pseudorange multipath at each site was the TEQC software (Estey and Meertens, 1999). It computes the MP1 and MP2 linear combinations using both pseudorange and carrier phase data to eliminate the effects of station clocks, satellite clocks, tropospheric delay, and ionospheric delay:

$$MP1 \equiv P_1 - \left(1+\frac{2}{\alpha-1}\right)L_1 + \left(\frac{2}{\alpha-1}\right)L_2 = M_1 + B_1 - \left(1+\frac{2}{\alpha-1}\right)m_1 + \left(\frac{2}{\alpha-1}\right)m_2 \qquad (1)$$

where $B_1 \equiv -\left(1+\frac{2}{\alpha-1}\right)n_1\lambda_1 + \left(\frac{2}{\alpha-1}\right)n_2\lambda_2$, and $\alpha = \frac{f_1^2}{f_2^2}$

$$MP2 \equiv P_2 - \left(\frac{2\alpha}{\alpha-1}\right)L_1 + \left(\frac{2\alpha}{\alpha-1}-1\right)L_2 = M_2 + B_2 - \left(\frac{2\alpha}{\alpha-1}\right)m_1 + \left(\frac{2\alpha}{\alpha-1}-1\right)m_2 \qquad (2)$$

where $B_2 \equiv -\left(\frac{2\alpha}{\alpha-1}\right)n_1\lambda_1 + \left(\frac{2\alpha}{\alpha-1}-1\right)n_2\lambda_2$.

In equations (1) and (2) P_1 and P_2 represent the dual-frequency pseudorange observations, L_1 and L_2 represent the dual-frequency carrier phase observations, and m_1 and m_2 represents the dual-frequency carrier phase multipath. The MP1 and MP2 quantities vary in time mostly due to M_i and B_i , where M_i is the pseudorange multipath for frequency i = 1, 2 and B_i is a bias related to the L1 and L2 integer carrier phase ambiguities, n_1 and n_2 . TEQC carefully monitors cycle slips and their effect on the bias terms B_i. In practice, the constant part of MP1 and MP2 (for 30-second data, the average over the last 50 epochs) is removed so what TEQC actually reports is the root mean square (RMS) variation of MP1 and MP2 for each satellite, as well as a mean RMS for all satellites. In MP1 and MP2 there remains the effects of pseudorange noise (< 25 cm), carrier phase multipath (< 7 cm), and carrier phase noise (< 2 mm) but these are much smaller in size compared to the pseudorange multipath (which can be as large as 10 to 15 meters at low elevation angles). Receivers such as the Ashtech Z-12, the Ashtech UZ-12, and the Allen Osborne ACT-family of receivers, collect three types of pseudoranges: C1 (C/A code), P1 (P-code), and P2 (P-code). When computing MP1, TEQC selects the more accurate P1 observable over the C1 observable. In rare instances, if P1 is unavailable in a RINEX file at a certain epoch then TEQC will use C1 instead. C1 is more affected by multipath than P1. If TEQC had been forced to use only the C1 observable (by removing all P1 observations from certain RINEX files) then the MP1 RMS values reported here for those 190 or so receivers that collect both C1 and P1 would have been significantly larger (e.g., the daily RMS values for the DGPS/NDGPS sites would have been increased by about 10 to 40 percent).

2 Description of the Study

The TEQC software was run using RINEX files, each spanning 24 hours with a 30 second sampling rate, for 390+ stations from Day 240, 2001, to Day 240, 2002. Every third day was used for a total of about 120 days. For each day and each station, TEQC was run three times, using elevation mask angles of 10°, 20°, and 60°. The overall RMS for MP1 and MP2 from each run was included only if the site had at least 22 hours of data with 90% of the data available. If an antenna or receiver was replaced at a site, then the site was afterwards counted as a new station. If a station had fewer than three acceptable days, it was ignored (this 3-day threshold was kept small for the sake of new stations recently added to the network). These daily RMS values were then combined into a yearly mean RMS for each station, and the associated sample standard deviations were computed. The yearly mean RMS values were computed for MP1 and MP2 for each of the three elevation mask angles. This was done to show which stations might be more affected by low-elevation-angle reflectors and which stations might be more affected by high-elevation-angle reflectors. The yearly mean RMS values and the sample standard deviations for all 390+ sites are shown plotted highest to lowest (most affected to least affected) in Figures 1 through 6. The 30 most affected sites are also listed in each figure along with their receiver type, antenna type, and firmware version. Since GPS users often use elevation cutoff angles of 15° or 20° when processing data, we expect that most readers will find the 20° elevation mask results the most interesting.

In the list of the most affected sites in Figure 3, one can see that there are several maritime Differential GPS and Nationwide Differential GPS (DPGS/NDGPS) sites with a very large MP1 RMS values (these sites are the ones labeled as using ASHTECH Z-XII3 receivers and ASH700829.3 SNOW antennas). These same sites are present in Figures 5 and 6, which indicates that they are being affected by high-elevation-angle multipath. This is most likely due to transmission towers located nearby which are used to broadcast correctors to Differential GPS (DGPS) users (Wolfe et al. 2000). The photographs in Figures 7 through 9 show some examples of these towers. To further verify that high-elevation-angle multipath was occurring, we plotted the epoch-by-epoch variation of MP1 and MP2 for several of these stations using skyplots. Figures 18 and 19 show an example for station CHA2; skyplots for other DPGS/NDGPS stations such as RIS2 and RED1 showed similar high-elevation-angle multipath. For contrast, Figures 20 and 21 show the MP1 and MP2 skyplots for one of the least affected stations in the network, OKEE. Figures 18 and 19 clearly show that the severely affected DPGS/NDGPS sites seem to be much more affected in MP1 than MP2 (these figures were created using the P1 and P2 observables, respectively). Again, if Figure 18 had been computed using the C1 observable instead of P1, the average magnitude of the MP1 multipath variations would have been about 40 percent larger. These skyplots were created using the epoch-by-epoch multipath variations found in the *.mp1 and *.mp2 plot files output by TEQC.

The list in Figure 4 shows that for MP2, the 30 most affected stations now include many non-DPGS/NDGPS sites. A few of these sites are pictured in Figures 13 through 17; one can see that these photographs show no evidence of major reflectors. Figure 12 shows a picture of the WAAS antenna used at stations ZAB1, ZAB2, ZOA1, ZOA2, and ZJX1. Figure 11 shows the MP2 day-to-day variation for some of these non- DPGS/NDGPS sites. The beginning of 2002 is marked by the light blue line at MJD 52275.

Figures 22(a) and 22(b) plot the yearly mean MP1 RMS values versus the yearly mean MP2 RMS values for the 20° elevation mask. These figures show the yearly mean values for those sites which use the 12 most common Receiver/Antenna combinations in the network. In the legend in Figure 22(a), the numbers in parentheses represent the number of sites in the network that use each particular receiver/antenna combination. Table 1 and Table 2 show the 40 least affected sites for the 20° elevation mask, for MP1 and MP2, respectively. For the sake of brevity, we have shown only the 30 most affected sites (for all three mask angles) and the 40 least affected sites (for the 20°mask angle). A complete list of all 390+ sites, for MP1 and MP2, and for all three elevation masks, will be published in a later report.

3 Results

The lists in Figures 5 and 6 show that the DPGS/NDGPS sites (those sites that use the ASHTECH Z-XII3 receiver and ASH700829.3 SNOW antenna) are most affected by high-elevation-angle reflectors. Figures 7 through 9 show photographs of some of these severely affected sites. As shown by Figures 18 and 19, these high-reflector sites tend to be much more affected in MP1 than in MP2. However, the least affected DPGS/NDGPS sites in the network do not exhibit this interesting behavior, as shown in Figure 22(b) by the Z symbols in the lower left corner. Although they are not shown in Tables 1 and 2, we noticed that the stations recently installed in Myton, Utah, and Pueblo, Colorado (which use pillars and choke ring antennas) are now among the best DGPS/NDGPS sites. Figures 3 through 6 show that two DGPS/NDGPS stations, LOU2 and YOU2, exhibit much larger MP1 and MP2 numbers than any other DPGS/NDGPS site. Station LOU2 as shown in Figure 10 is mostly in the clear, with a small transmission tower located about 150 feet to the west. The picture of YOU2 in Figure 14 likewise seems to have no major obstructions or reflectors nearby. Because these two stations are so much worse than any other DPGS/NDGPS site, we expect that perhaps equipment problems are to blame. Figures 3 and 4 show that their companion stations, YOU1 and LOU1, have high MP1 values but are not much affected in MP2.

Figure 4 shows that for MP2, the non- DPGS/NDGPS sites have the largest RMS values. Stations LUMC and COCD are actually the same station (station COCD was renamed to LUMC). This station is shown in Figure 15. It is interesting to note that the Trimble receivers in the Figure 4 list are accompanied by a mixture of choke ring antennas and ground plane antennas. Figure 11 shows the variation of the daily MP2 values for 10 of these highly affected non- DPGS/NDGPS stations. Stations SLCU (U) seems to have some very dramatic day-to-day variations, while the WAAS stations ZAB1 (Z) and ZOA1 (X) show very little deviation from one day to the next. In Figure 11, the grouping of some days in a systematic manner may be related to temperature variations and/or precipitation at a site. Photographs of a few of these non-DPGS/NDGPS sites (ANTO, LUMC, FDTC, and GNAA) are shown in Figures 13-17.

Figures 18, 19, 20, and 21 show examples of the range of multipath errors that can be found in the network. Station CHA2 is one of the most severely affected stations, and OKEE is one of the least affected. Looking closely at the photograph in Figure 7 for stations CHA1 and CHA2 one can see that the transmission tower has been placed midway between the two GPS antennas. Station CHA2 is on the left and probably receives reflections from both the transmission tower (which rises up to a 75° angle when viewed from CHA2) and from the lighthouse in the background. It is interesting to note in Figure 18 how large (5-6 meters) the MP1 variations become, even above a 60° elevation angle (note that Figure 18 was computed using only the P1 observable). These skyplots have proven to be a very useful tool for investigating individual sites.

Like Figures 18 and 19, Figure 22(a) shows how much more MP1 is affected versus MP2 for the severely affected DPGS/NDGPS sites. Figure 22(b) is a very interesting plot in that it shows how the newer receiver technology (such as the Ashtech UZ-12, Leica RS500, and Trimble 5700) has dramatically decreased the amounts of pseudorange multipath. It also shows how several of the DGPS/NDGPS sites and all of the WAAS sites seem to be among those most affected by pseudorange multipath (the Federal Aviation Administration will soon upgrade the antennas at all WAAS sites). It is also interesting to note how the older generation Trimble receivers seem to be much more affected in MP2 than MP1. The reader needs to keep in mind, however, that this figure does not take into account the differences in the multipath environment at the sites. It is possible that a well-performing receiver/antenna could have been consistently deployed at very poor site locations, and vice-versa. The reader should also keep in mind that newer receivers that do a good job mitigating pseudorange multipath may not necessarily improve the carrier phase multipath.

Tables 1 and 2 list the 40 least affected sites in the CORS network, for MP1 and MP2, respectively (using the 20°elevation mask). They are listed in order from worst to best (most affected to least affected). The Leica RS500 receivers from the state network in Michigan occupy the last 16 lines in Table 1. In Table 2, above the Leica RS500 sites, are several sites from the state network in Ohio which use the Trimble 5700 receiver and the TRM29659.00 antenna. For antenna mounts, these Ohio sites used very stable concrete pillars which extend 10 feet below the ground and 8 feet above the ground. Figures 23 and 24 show examples of the Michigan and Ohio antenna mounts. Table 2 also lists several other good sites such as TSEA (Alaska), MINS (California), PUC1 (Utah), JAMA (Jamaica), UIUC (Illinois), ATL1 (Georgia), which use various different receiver/antenna combinations to achieve excellent results.

4 Summary

To summarize, this initial study has identified several severely affected sites. Some of these sites are affected by large pseudorange multipath variations even at high elevation angles. The study has also pointed out the success stories; those networks in Ohio and Michigan where a combination of new receiver/antenna technology, excellent antenna mounting, and good site location has dramatically lowered the effects of pseudorange multipath. The plots shown in Figures 18 through 20 show how examining the epoch-by-epoch variations of the MP1 and MP2 values with respect to azimuth and elevation can be a useful tool for analyzing individual sites. And finally the comparison of different receiver/antenna combinations as shown in Figure 22(b) would seem to indicate that for several manufacturers, the newer generation receivers do a much better job of mitigating pseudorange multipath than their predecessors. The known existence of high-elevation-angle reflectors at some DGPS/NDGPS sites would make it difficult to use carrier phase calibration techniques such as those described by Wanninger and May (2001) for the National CORS Network. However, with knowledge of which sites are severely affected by multipath, one can experiment with other in-situ carrier phase calibration techniques to see how well they perform at these very challenging sites.

Figure 1.

Variation of MP1 RMS (380 stations sorted highest to lowest) 10 Elev.Cutoff

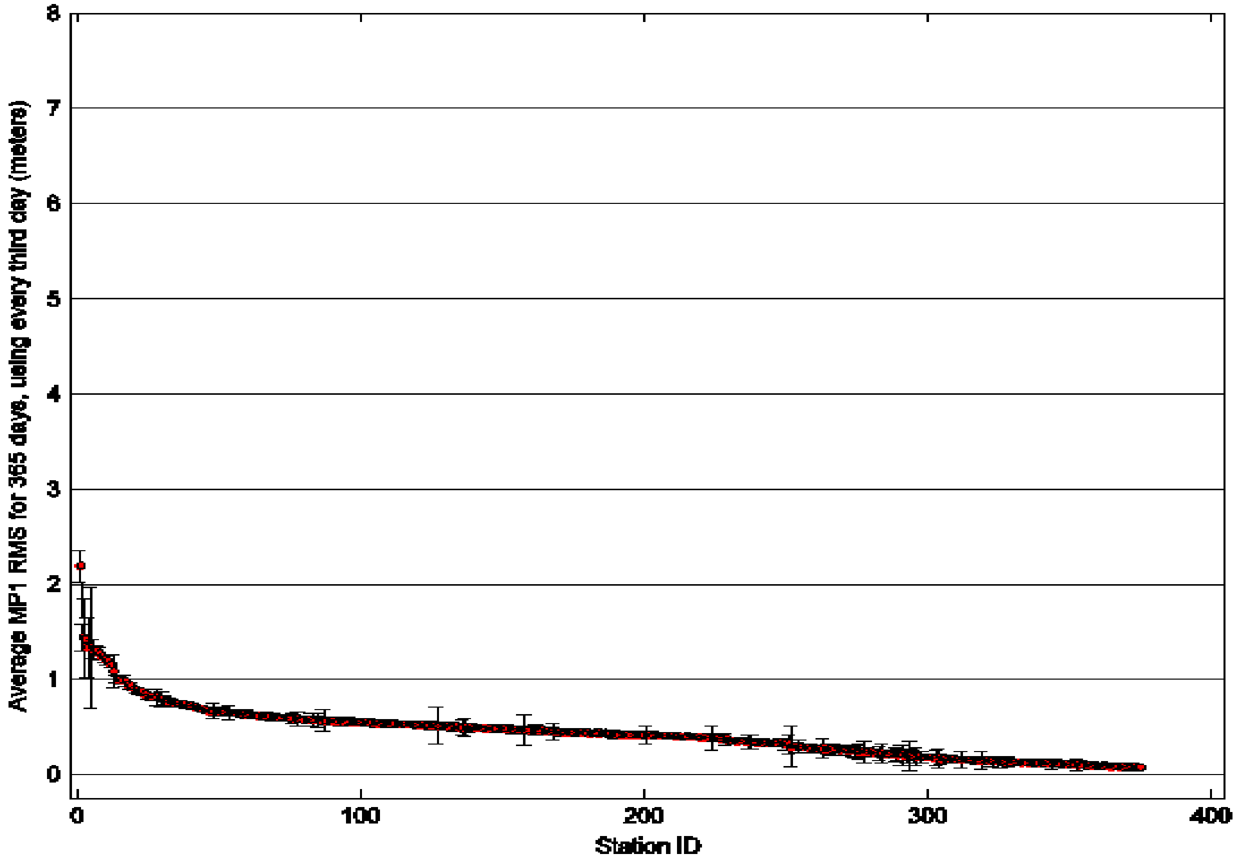

Rank	MP1	StdDev	Site	#Days	Receiver Type	Antenna Type	Firmware
1	2.1881	0.1677	cha2	93	ASHTECH Z-XII3	ASH700829.3 SNOW	RC00
2	1.4413	0.1370	kyw2	95	ASHTECH Z-XII3	ASH700829.3 SNOW	RC00
3	1.4257	0.4211	ris2	30	ASHTECH Z-XII3	ASH700829.3 SNOW	RC00
4	1.3360	0.3161	ris1	112	ASHTECH Z-XII3	ASH700829.3 SNOW	RC00
5	1.3325	0.6330	pur2	4	ASHTECH Z-XII3	ASH700829.3 SNOW	RC00
6	1.3109	0.0979	you1	105	ASHTECH Z-XII3	ASH700829.3 SNOW	RC00
7	1.2955	0.0474	red1	106	ASHTECH Z-XII3	ASH700829.3 SNOW	RC00
8	1.2693	0.0683	kew1	107	ASHTECH Z-XII3	ASH700829.3 SNOW	RC00
9	1.2356	0.0226	kok2	41	ASHTECH Z-XII3	ASH700829.3 SNOW	RC00
10	1.2080	0.0357	mem1	15	ASHTECH Z-XII3	ASH700829.3 SNOW	RC00
11	1.1836	0.0361	red2	11	ASHTECH Z-XII3	ASH700829.3 SNOW	RC00
12	1.1525	0.0242	chl1	40	ASHTECH Z-XII3	ASH700829.3 SNOW	RC00
13	1.0855	0.1770	lou1	110	ASHTECH Z-XII3	ASH700829.3 SNOW	RC00
14	1.0017	0.0383	omh1	109	ASHTECH Z-XII3	ASH700829.3 SNOW	RC00
15	0.9941	0.0286	stl3	51	ASHTECH Z-XII3	ASH700829.3 SNOW	RC00
16	0.9873	0.0309	arp3	112	ASHTECH Z-XII3	ASH700829.3 SNOW	RC00
17	0.9828	0.0578	por4	103	ASHTECH Z-XII3	ASH700829.3 SNOW	1C80
18	0.9413	0.0178	zab1	16	NovWAAS	MPL_WAAS_2224NW DOME	
19	0.9331	0.0330	zab2	16	NovWAAS	MPL_WAAS_2224NW DOME	
20	0.8935	0.0132	zoa2	17	NovWAAS	MPL_WAAS_2224NW DOME	
21	0.8900	0.0264	pltk	26	ASHTECH Z-XII3	ASH701933A_M	CD00
22	0.8706	0.0222	zoa1	17	NovWAAS	MPL_WAAS_2224NW DOME	
23	0.8694	0.0293	mlf1	110	ASHTECH Z-XII3	ASH700829.3 SNOW	RC00
24	0.8471	0.0221	arp2	7	ASHTECH Z-XII3	ASH700829.3 SNOW	RC00
25	0.8182	0.0298	cha1	103	ASHTECH Z-XII3	ASH700829.3 SNOW	RC00
26	0.8175	0.0270	kew2	51	ASHTECH Z-XII3	ASH700829.3 SNOW	RC00
27	0.8118	0.0389	cht2	11	ASHTECH Z-XII3	ASH700829.3 SNOW	RC00
28	0.8115	0.0839	sag1	106	ASHTECH Z-XII3	ASH700829.3 SNOW	RC00
29	0.8060	0.0261	omh2	5	ASHTECH Z-XII3	ASH700829.3 SNOW	RC00
30	0.7873	0.0839	cena	66	TRIMBLE 4000SSI	TRM22020.00+GP DOME	7.12

Figure 2.

Variation of MP2 RMS (380 stations sorted highest to lowest) 10 Elev.Cutoff

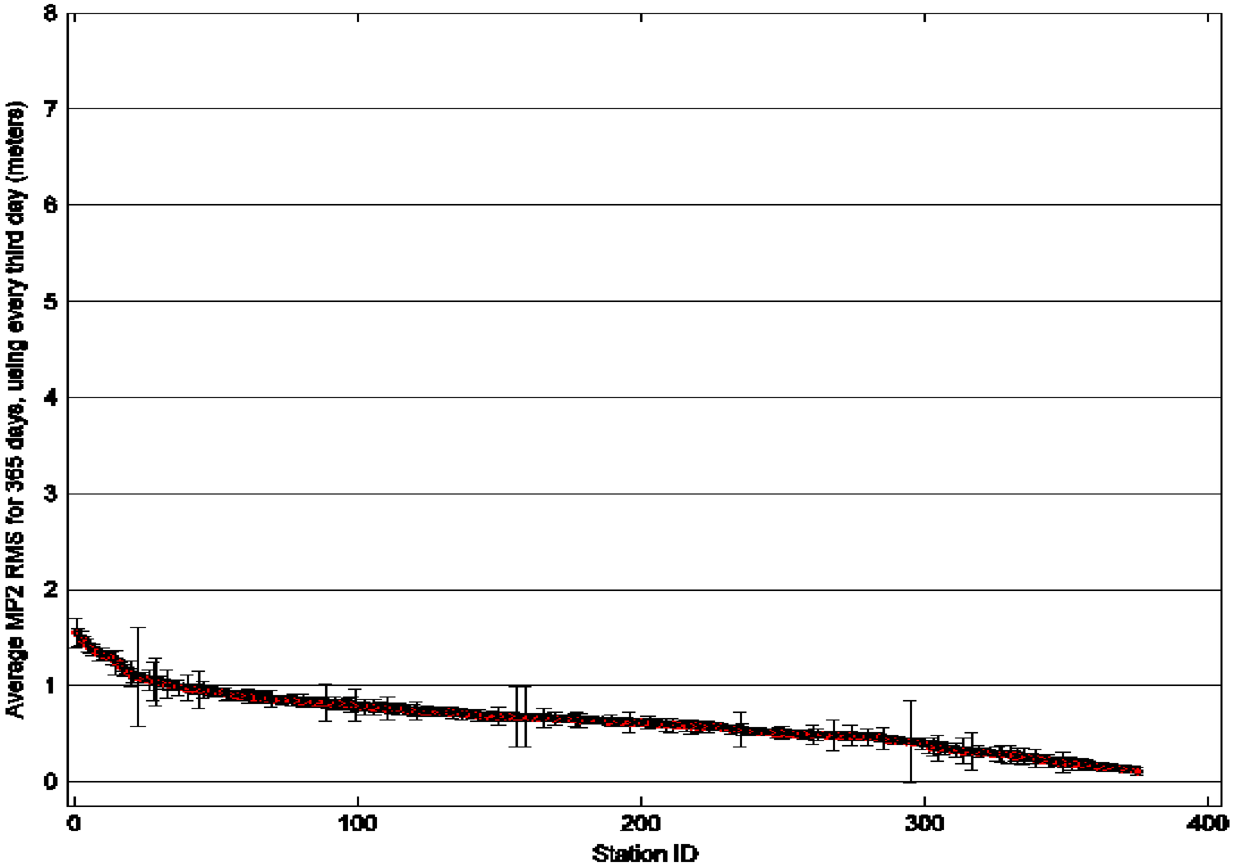

Rank	MP2	StdDev	Site	#Days	Receiver Type	Antenna Type		Firmware
1	1.5491	0.1515	sc00	69	TRIMBLE 4700	TRM29659.00	SCIT	1.35
2	1.4967	0.0945	lumc	3	TRIMBLE 4000SSI	TRM29659.00		7.19A
3	1.4908	0.0707	fdtc	72	TRIMBLE 4000SSI	TRM29659.00		7.32
4	1.4655	0.0424	egan	93	TRIMBLE 4000SSE	TRM29659.00		7.29
5	1.4187	0.0676	cocd	16	TRIMBLE 4000SSI	TRM29659.00		7.19A
6	1.3929	0.0502	zoa1	17	NovWAAS	MPL_WAAS_2224NW	DOME	
7	1.3725	0.0622	garl	117	TRIMBLE 4000SSI	TRM29659.00	SCIS	7.19a
8	1.3612	0.0260	zab1	16	NovWAAS	MPL_WAAS_2224NW	DOME	
9	1.3247	0.0688	corb	100	TRIMBLE 4000SSI	AOAD/M_T		7.29
10	1.3227	0.0644	kels	100	TRIMBLE 4000SSI	TRM29659.00	UNAV	7.19
11	1.3180	0.0502	cosa	41	TRIMBLE 4000SSE	TRM22020.00+GP		7.24
12	1.3011	0.0317	anto	53	TRIMBLE 4000SSE	TRM22020.00+GP		7.29
13	1.2863	0.0287	zab2	16	NovWAAS	MPL_WAAS_2224NW	DOME	
14	1.2833	0.0724	burn	118	TRIMBLE 4000SSI	TRM29659.00	UNAV	7.29
15	1.2417	0.1254	zjx1	18	NovWAAS	MPL_WAAS_2224NW	DOME	
16	1.2376	0.0291	zoa2	17	NovWAAS	MPL_WAAS_2224NW	DOME	
17	1.1962	0.0473	kjun	61	TRIMBLE 4000SSI	TRM29659.00		7.19A
18	1.1578	0.0645	mawy	109	TRIMBLE 4000SSI	TRM29659.00	DOME	7.15
19	1.1541	0.0339	mana	110	TRIMBLE 4000SSI	TRM29659.00	UNAV	7.29
20	1.1238	0.1285	fred	108	TRIMBLE 4000SSI	TRM29659.00	SCIS	7.29
21	1.1025	0.0683	cola	105	TRIMBLE 4000SSI	TRM29659.00		7.28
22	1.0943	0.0287	esti	99	TRIMBLE 4000SSI	TRM29659.00	UNAV	7.29
23	1.0875	0.5168	pur2	4	ASHTECH Z-XII3	ASH700829.3	SNOW	RCOO
24	1.0824	0.0561	seat	100	TRIMBLE 4000SSI	TRM29659.00	DOME	7.19
25	1.0677	0.0387	blmm	22	TRIMBLE 4000SSI	TRM33429.20+GP		7.31
26	1.0634	0.0284	red1	106	ASHTECH Z-XII3	ASH700829.3	SNOW	RC00
27	1.0507	0.1070	cabl	120	TRIMBLE 4000SSI	TRM29659.00		7.26
28	1.0438	0.1981	slcu	39	TRIMBLE 4000SSI	TRM33429.00+GP		7.19
29	1.0391	0.2426	pabh	102	TRIMBLE 4000SSI	TRM29659.00		7.26
30	1.0389	0.0352	adks	9	TRIMBLE 4000SSI	TRM29659.00		7.22

Figure 3.
Variation of MP1 RMS (400 stations sorted highest to lowest) 20 Elev.Cutoff

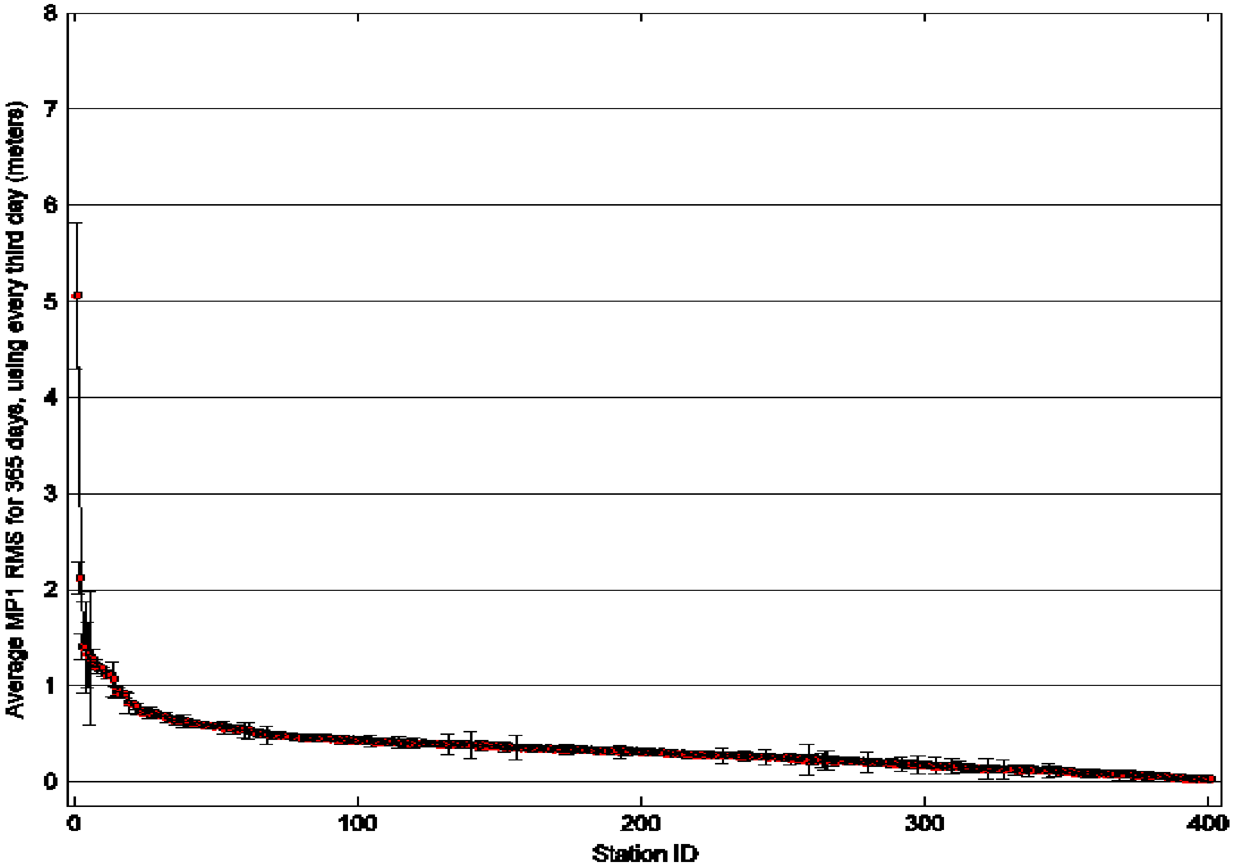

Rank	MP1	StdDev	Site	#Days	Receiver Type		Antenna Type		Firmware
1	5.0575	0.7628	lou2	4	ASHTECH	Z-XII3	ASH700829.3	SNOW	RC00
2	2.1156	0.1629	cha2	93	ASHTECH	Z-XII3	ASH700829.3	SNOW	RC00
3	1.4062	0.1362	kyw2	96	ASHTECH	Z-XII3	ASH700829.3	SNOW	RC00
4	1.3950	0.4737	ris2	30	ASHTECH	Z-XII3	ASH700829.3	SNOW	RC00
5	1.3205	0.3421	ris1	112	ASHTECH	Z-XII3	ASH700829.3	SNOW	RC00
6	1.2900	0.6987	pur2	4	ASHTECH	Z-XII3	ASH700829.3	SNOW	RC00
7	1.2738	0.0997	you1	108	ASHTECH	Z-XII3	ASH700829.3	SNOW	RC00
8	1.2014	0.0713	kew1	110	ASHTECH	Z-XII3	ASH700829.3	SNOW	RC00
9	1.1857	0.0194	kok2	47	ASHTECH	Z-XII3	ASH700829.3	SNOW	RC00
10	1.1706	0.0286	mem1	16	ASHTECH	Z-XII3	ASH700829.3	SNOW	RC00
11	1.1190	0.0226	chl1	40	ASHTECH	Z-XII3	ASH700829.3	SNOW	RC00
12	1.1162	0.0521	red1	106	ASHTECH	Z-XII3	ASH700829.3	SNOW	RC00
13	1.1046	0.0296	red2	13	ASHTECH	Z-XII3	ASH700829.3	SNOW	RC00
14	1.0639	0.1838	lou1	111	ASHTECH	Z-XII3	ASH700829.3	SNOW	RC00
15	0.9340	0.0589	por4	103	ASHTECH	Z-XII3	ASH700829.3	SNOW	1C80
16	0.9338	0.0446	omh1	110	ASHTECH	Z-XII3	ASH700829.3	SNOW	RC00
17	0.9041	0.0290	stl3	51	ASHTECH	Z-XII3	ASH700829.3	SNOW	RC00
18	0.9033	0.0318	arp3	115	ASHTECH	Z-XII3	ASH700829.3	SNOW	RC00
19	0.8163	0.1103	tlka	84	TRIMBLE	4000SSI	TRM22020.00+GP	DOME	7.19A
20	0.8102	0.0223	wnfl	57	TRIMBLE	4000SSI	TRM22020.00+GP		7.28
21	0.8100	0.0167	zab1	16	NovWAAS		MPL_WAAS_2224NW	DOME	
22	0.7769	0.0309	zab2	16	NovWAAS		MPL_WAAS_2224NW	DOME	
23	0.7242	0.0273	mlf1	113	ASHTECH	Z-XII3	ASH700829.3	SNOW	RC00
24	0.7227	0.0231	kew2	52	ASHTECH	Z-XII3	ASH700829.3	SNOW	RC00
25	0.7218	0.0095	zoa2	17	NovWAAS		MPL_WAAS_2224NW	DOME	
26	0.7185	0.0241	jxvl	27	ASHTECH	Z-XII3	ASH701933A_M		CD00
27	0.7178	0.0607	gnaa	98	TRIMBLE	4000SSI	TRM22020.00+GP	DOME	7.28
28	0.7103	0.0440	det1	112	ASHTECH	Z-XII3	ASH700829.3	SNOW	RC00
29	0.7027	0.0312	cha1	104	ASHTECH	Z-XII3	ASH700829.3	SNOW	RC00
30	0.6947	0.0248	zoa1	17	NovWAAS		MPL_WAAS_2224NW	DOME	

Figure 4.

Variation of MP2 RMS (400 stations sorted highest to lowest) 20 Elev.Cutoff

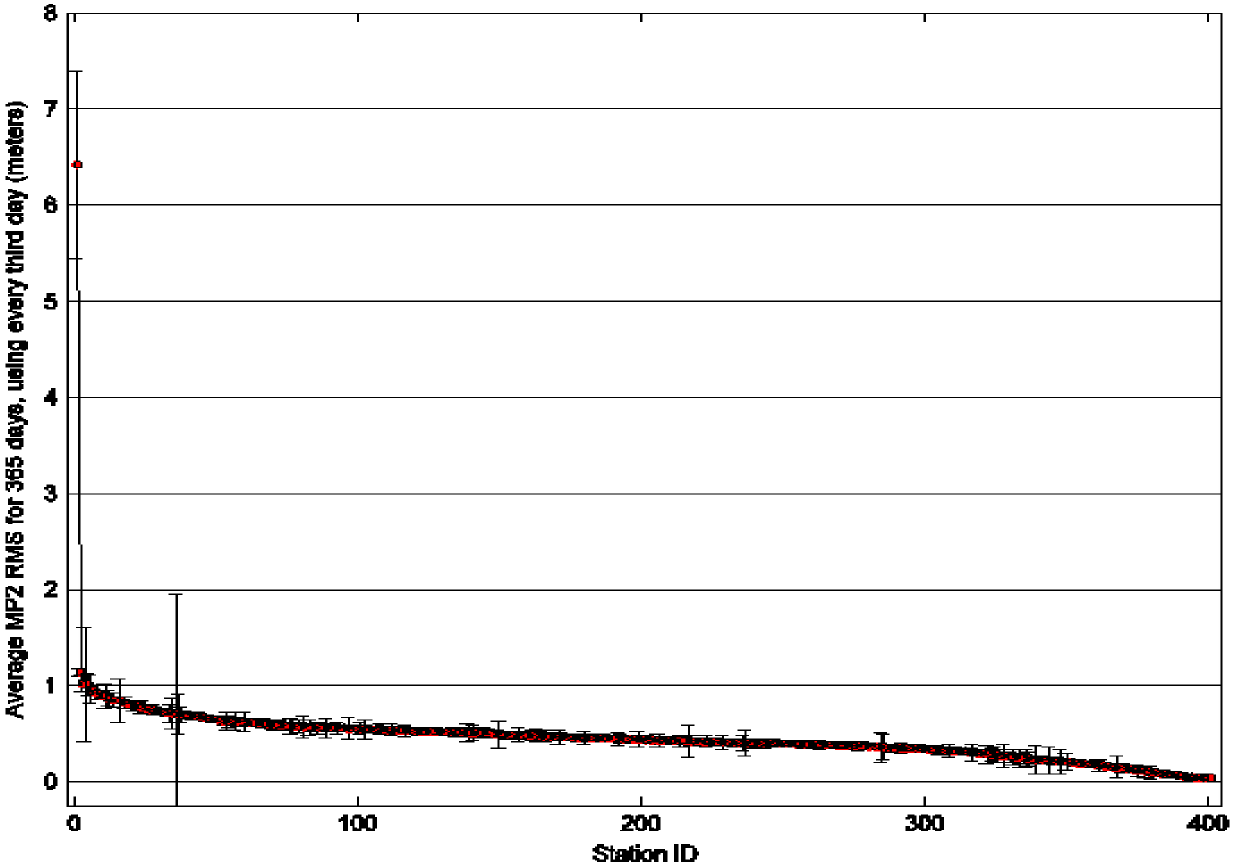

Rank	MP2	StdDev	Site	#Days	Receiver Type	Antenna Type		Firmware
1	6.4200	0.9769	lou2	4	ASHTECH Z-XII3	ASH700829.3	SNOW	RC00
2	1.1371	0.0395	lumc	52	TRIMBLE 4000SSI	TRM29659.00		7.19A
3	1.0242	0.0908	cocd	19	TRIMBLE 4000SSI	TRM29659.00		7.19A
4	1.0125	0.5920	pur2	4	ASHTECH Z-XII3	ASH700829.3	SNOW	RC00
5	1.0115	0.1199	tlka	84	TRIMBLE 4000SSI	TRM22020.00+GP	DOME	7.19A
6	0.9601	0.1458	sc00	69	TRIMBLE 4700	TRM29659.00	SCIT	1.35
7	0.9544	0.0096	zab1	16	NovWAAS	MPL_WAAS_2224NW	DOME	
8	0.9230	0.0340	wnfl	57	TRIMBLE 4000SSI	TRM22020.00+GP		7.28
9	0.9027	0.0427	egan	114	TRIMBLE 4000SSE	TRM29659.00		7.29
10	0.8988	0.0297	red1	106	ASHTECH Z-XII3	ASH700829.3	SNOW	RC00
11	0.8863	0.1224	fdtc	106	TRIMBLE 4000SSI	TRM29659.00		7.32
12	0.8679	0.0796	gnaa	98	TRIMBLE 4000SSI	TRM22020.00+GP	DOME	7.28
13	0.8575	0.0124	zab2	16	NovWAAS	MPL_WAAS_2224NW	DOME	
14	0.8520	0.0755	anto	86	TRIMBLE 4000SSE	TRM22020.00+GP		7.29
15	0.8447	0.0162	zoa1	17	NovWAAS	MPL_WAAS_2224NW	DOME	
16	0.8435	0.2232	slcu	72	TRIMBLE 4000SSI	TRM33429.00+GP		7.19
17	0.8372	0.0141	zjx1	18	NovWAAS	MPL_WAAS_2224NW	DOME	
18	0.8213	0.0543	ris2	30	ASHTECH Z-XII3	ASH700829.3	SNOW	RC00
19	0.8124	0.0130	zoa2	17	NovWAAS	MPL_WAAS_2224NW	DOME	
20	0.8027	0.0388	okom	94	TRIMBLE 4000SSI	TRM33429.00+GP		7.29
21	0.7926	0.0553	cosa	43	TRIMBLE 4000SSE	TRM22020.00+GP		7.24
22	0.7861	0.0238	kjun	62	TRIMBLE 4000SSI	TRM29659.00		7.19A
23	0.7847	0.0361	blmm	92	TRIMBLE 4000SSI	TRM33429.20+GP		7.31
24	0.7706	0.0685	sag1	110	ASHTECH Z-XII3	ASH700829.3		RC00
25	0.7612	0.0424	chzz	51	TRIMBLE 4000SSI	TRM29659.00		7.29
26	0.7609	0.0411	mem2	112	ASHTECH Z-XII3	ASH700829.3	SNOW	RC00
27	0.7494	0.0422	ccpt	62	TRIMBLE 5700	TRM41249.00		1.04
28	0.7457	0.0540	pur3	100	ASHTECH Z-XII3	ASH700829.3	SNOW	RC00
29	0.7362	0.0156	red2	13	ASHTECH Z-XII3	ASH700829.3	SNOW	RC00
30	0.7341	0.0182	jxvl	27	ASHTECH Z-XII3	ASH701933A_M		CD00

Figure 5.

Variation of MP1 RMS (400 stations sorted highest to lowest) 60 Elev.Cutoff

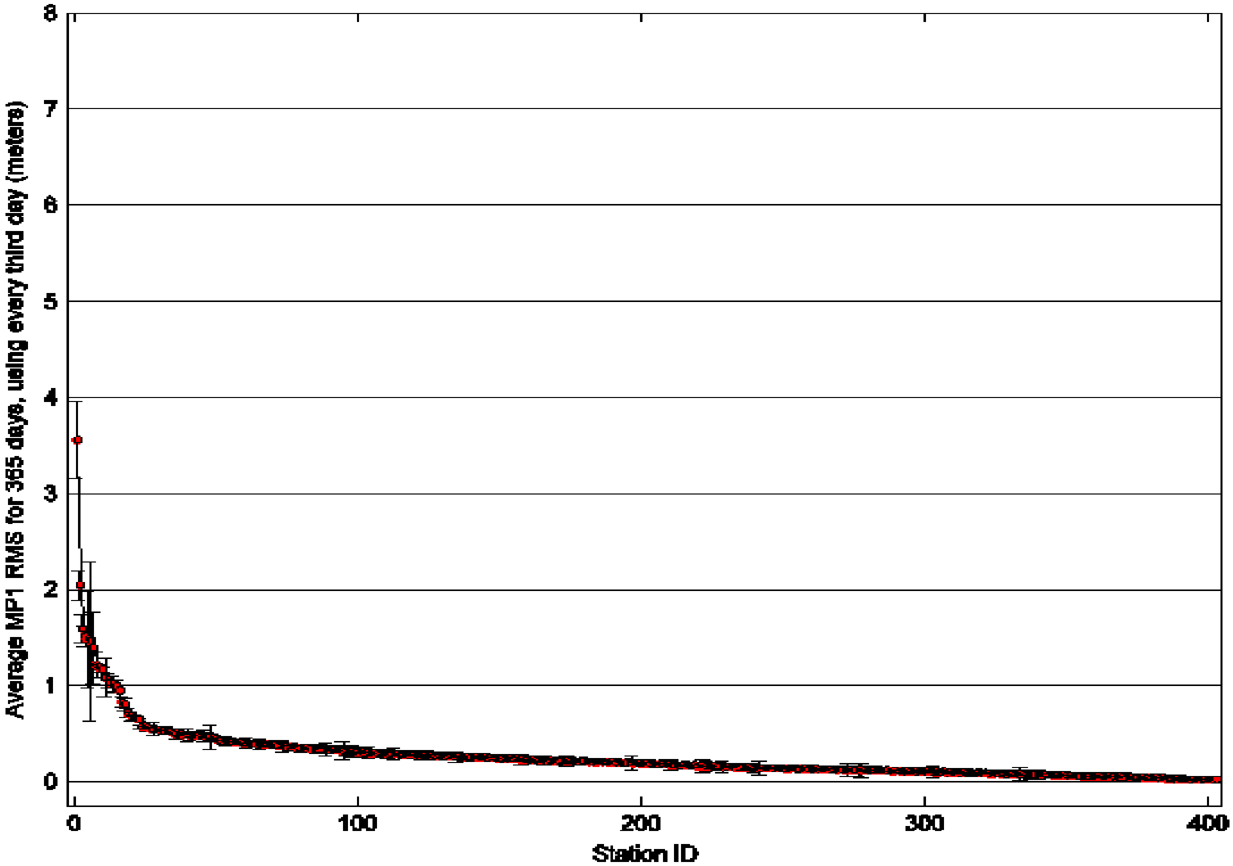

Rank	MP1	StdDev	Site	#Days	Receiver Type	Antenna Type		Firmware
1	3.5537	0.3998	lou2	16	ASHTECH Z-XII3	ASH700829.3	SNOW	RC00
2	2.0400	0.1539	you2	7	ASHTECH Z-XII3	ASH700829.3	SNOW	RC00
3	1.5927	0.1421	cha2	93	ASHTECH Z-XII3	ASH700829.3	SNOW	RC00
4	1.5070	0.1058	you1	108	ASHTECH Z-XII3	ASH700829.3	SNOW	RC00
5	1.4757	0.5031	ris2	30	ASHTECH Z-XII3	ASH700829.3	SNOW	RC00
6	1.4575	0.8287	pur2	4	ASHTECH Z-XII3	ASH700829.3	SNOW	RC00
7	1.3882	0.3734	ris1	113	ASHTECH Z-XII3	ASH700829.3	SNOW	RC00
8	1.2132	0.1341	kyw2	95	ASHTECH Z-XII3	ASH700829.3	SNOW	RC00
9	1.1887	0.0294	mem1	16	ASHTECH Z-XII3	ASH700829.3	SNOW	RC00
10	1.1620	0.0251	chl1	40	ASHTECH Z-XII3	ASH700829.3	SNOW	RC00
11	1.0786	0.2019	lou1	111	ASHTECH Z-XII3	ASH700829.3	SNOW	RC00
12	1.0541	0.0738	kew1	109	ASHTECH Z-XII3	ASH700829.3	SNOW	RC00
13	1.0283	0.0255	red2	12	ASHTECH Z-XII3	ASH700829.3	SNOW	RC00
14	1.0154	0.0886	red1	105	ASHTECH Z-XII3	ASH700829.3	SNOW	RC00
15	0.9970	0.0625	por4	101	ASHTECH Z-XII3	ASH700829.3	SNOW	1C80
16	0.9483	0.0251	kok2	46	ASHTECH Z-XII3	ASH700829.3	SNOW	RC00
17	0.8246	0.0530	omh1	110	ASHTECH Z-XII3	ASH700829.3	SNOW	RC00
18	0.8034	0.0634	det1	112	ASHTECH Z-XII3	ASH700829.3	SNOW	RC00
19	0.7144	0.0450	stl3	52	ASHTECH Z-XII3	ASH700829.3	SNOW	RC00
20	0.6793	0.0518	arp3	113	ASHTECH Z-XII3	ASH700829.3	SNOW	RC00
21	0.6648	0.0270	kew2	52	ASHTECH Z-XII3	ASH700829.3	SNOW	RC00
22	0.6593	0.0246	vic2	14	ASHTECH Z-XII3	ASH700829.3	SNOW	RC05
23	0.6457	0.0181	chb2	7	ASHTECH Z-XII3	ASH700829.3	SNOW	RC00
24	0.5710	0.0185	chb1	112	ASHTECH Z-XII3	ASH700829.3	SNOW	RC00
25	0.5689	0.0255	whd1	105	ASHTECH Z-XII3	ASH700829.3	SNOW	RC00
26	0.5671	0.0439	mlf1	112	ASHTECH Z-XII3	ASH700829.3	SNOW	RC00
27	0.5529	0.0254	stp2	17	ASHTECH Z-XII3	ASH700829.3	SNOW	RC00
28	0.5465	0.0625	pur3	102	ASHTECH Z-XII3	ASH700829.3	SNOW	RC00
29	0.5443	0.0170	sal2	14	ASHTECH Z-XII3	ASH700829.3	SNOW	RC00
30	0.5366	0.0296	mob1	113	ASHTECH Z-XII3	ASH700829.3	SNOW	RC00

Figure 6.
Variation of MP2 RMS (400 stations sorted highest to lowest) 60 Elev.Cutoff

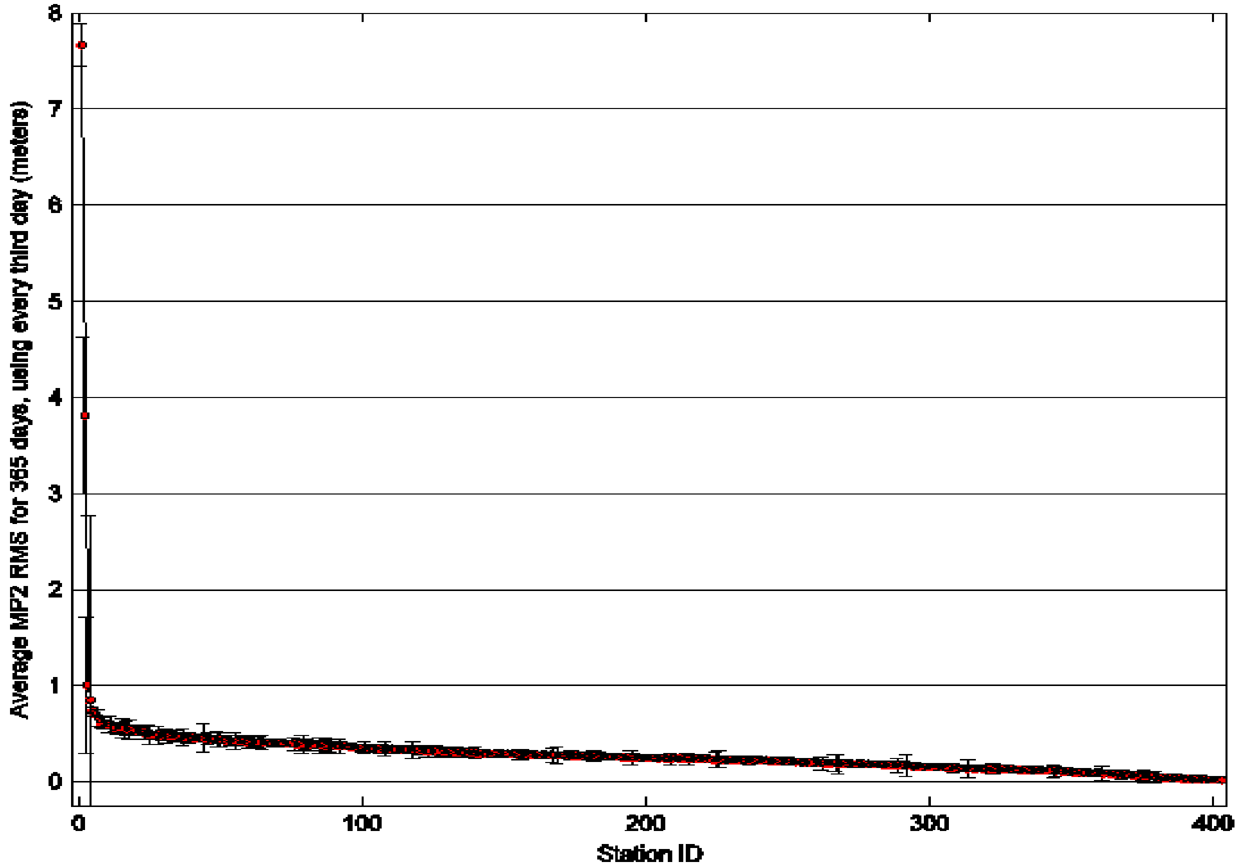

Rank	MP2	StdDev	Site	#Days	Receiver Type	Antenna Type		Firmware
1	7.6629	0.2206	you2	7	ASHTECH Z-XII3	ASH700829.3	SNOW	RC00
2	3.8125	0.8149	lou2	16	ASHTECH Z-XII3	ASH700829.3	SNOW	RC00
3	1.0050	0.7054	pur2	4	ASHTECH Z-XII3	ASH700829.3	SNOW	RC00
4	0.8446	1.9180	kokb	37	AOA SNR-12 ACT	AOAD/M_T		3.3.32.5
5	0.7386	0.0353	red1	105	ASHTECH Z-XII3	ASH700829.3	SNOW	RC00
6	0.6980	0.0233	kyw2	95	ASHTECH Z-XII3	ASH700829.3	SNOW	RC00
7	0.6627	0.0827	ris2	30	ASHTECH Z-XII3	ASH700829.3	SNOW	RC00
8	0.6220	0.0568	pur3	102	ASHTECH Z-XII3	ASH700829.3	SNOW	RC00
9	0.6060	0.0624	ris1	113	ASHTECH Z-XII3	ASH700829.3	SNOW	RC00
10	0.5975	0.0166	red2	12	ASHTECH Z-XII3	ASH700829.3	SNOW	RC00
11	0.5917	0.0848	anp1	104	ASHTECH Z-XII3	ASH700829.3	SNOW	RD00-1C19
12	0.5735	0.0224	kyw1	111	ASHTECH Z-XII3	ASH700829.3	SNOW	RC00
13	0.5621	0.0353	sal2	14	ASHTECH Z-XII3	ASH700829.3	SNOW	RC00
14	0.5572	0.0615	por4	101	ASHTECH Z-XII3	ASH700829.3	SNOW	1C80
15	0.5557	0.0431	chb2	7	ASHTECH Z-XII3	ASH700829.3	SNOW	RC00
16	0.5550	0.1014	acu1	48	ASHTECH Z-XII3	ASH700829.3	SNOW	RC00
17	0.5500	0.0745	lev2	13	ASHTECH Z-XII3	ASH700829.3	SNOW	RD00-1C19
18	0.5478	0.1022	lev1	97	ASHTECH Z-XII3	ASH700829.3	SNOW	RD00-1C19
19	0.5441	0.0479	mem2	111	ASHTECH Z-XII3	ASH700829.3	SNOW	RC00
20	0.5375	0.0558	kan1	109	ASHTECH Z-XII3	ASH700829.3	SNOW	RC00
21	0.5337	0.0113	chl1	40	ASHTECH Z-XII3	ASH700829.3	SNOW	RC00
22	0.5309	0.0260	acu2	22	ASHTECH Z-XII3	ASH700829.3	SNOW	RC00
23	0.5283	0.0508	sag1	109	ASHTECH Z-XII3	ASH700829.3	SNOW	RC00
24	0.4910	0.0436	vic1	110	ASHTECH Z-XII3	ASH700829.3	SNOW	RC00
25	0.4901	0.0989	bis1	109	ASHTECH Z-XII3	ASH700829.3	SNOW	RD00
26	0.4887	0.0164	kok2	46	ASHTECH Z-XII3	ASH700829.3	SNOW	RC00
27	0.4879	0.0145	stkr	98	ASHTECH Z-XII3	ASH700718B		1L00-1D04
28	0.4850	0.0965	pot3	107	ASHTECH Z-XII3	ASH700829.3	SNOW	RC00
29	0.4837	0.0477	mlf1	112	ASHTECH Z-XII3	ASH700829.3	SNOW	RC00
30	0.4836	0.0520	ais1	107	ASHTECH Z-XII3	ASH700829.3	SNOW	RC00

Figure 7. CHA1,CHA2 Charleston, SC

Figure 9. RED1,RED2 Reedy Pt. DE

Figure 8. RIS1,RIS2 Rock Island, IA

Figure 10. LOU1,LOU2 Louisville, KY

Figure 11. Daily MP2 values for 10 Selected Sites from Figure 4.

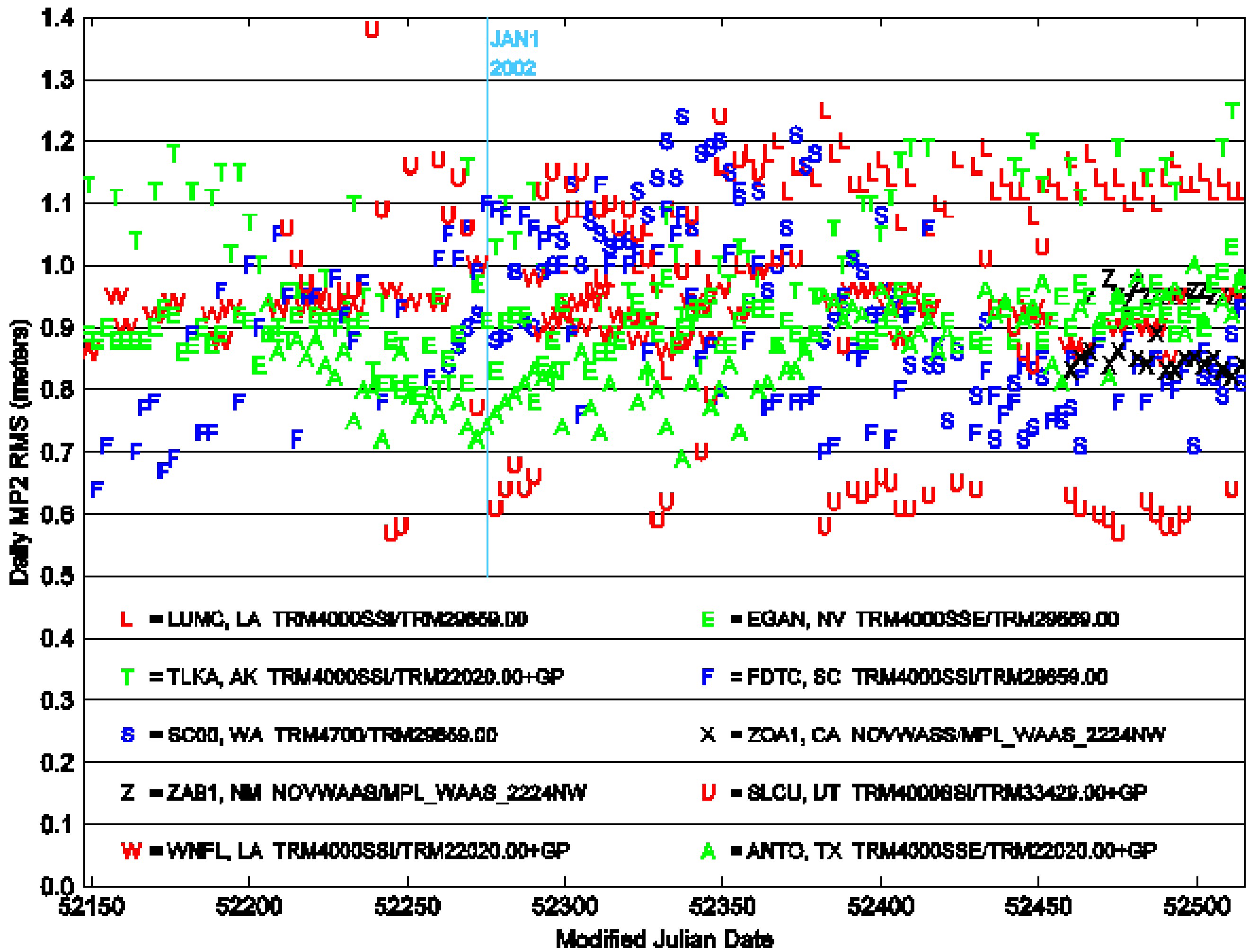

Figure 12. WAAS Antenna

Figure 15. LUMC, Lumcon, LA

Figure 13. ANTO, San Antonio, TX

Figure 16. FDTC, Florence, SC

Figure 14. YOU1, YOU2, Youngstown, NY

Figure 17. GNAA, Glennallen, AK

Figure 18. P1 Pseudorange Multipath at CHA2

Lat: 32.7575˚ Lon: -79.8432˚ Ell Ht: -27.4 (m)

GPS Time: Start 2002/08/28 00:00:00 Stop 2002/08/28 06:00:00

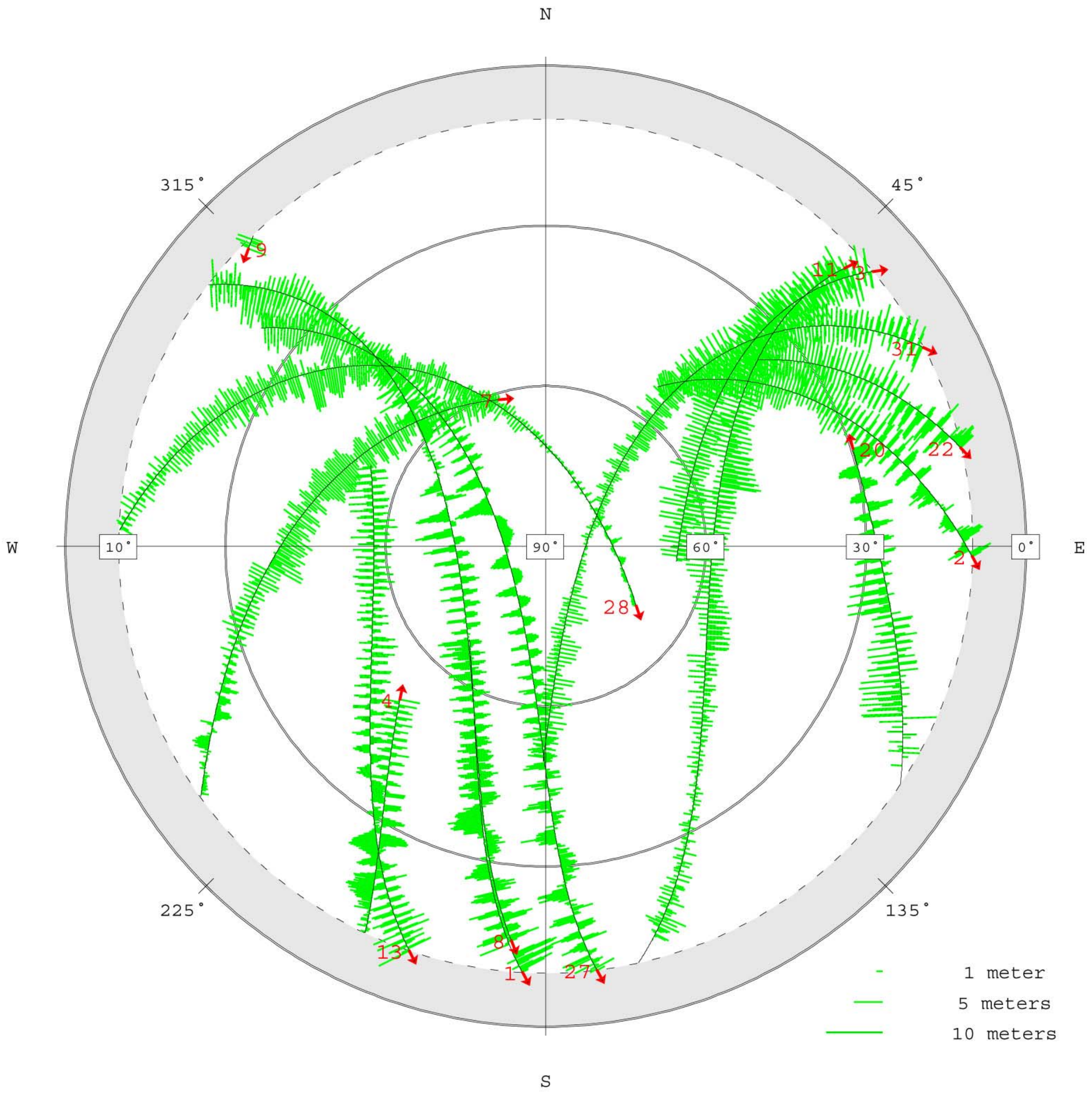

Figure 19. P2 Pseudorange Multipath at CHA2

Lat: 32.7575˚ Lon: -79.8432˚ Ell Ht: -27.4 (m)

GPS Time: Start 2002/08/28 00:00:00 Stop 2002/08/28 06:00:00

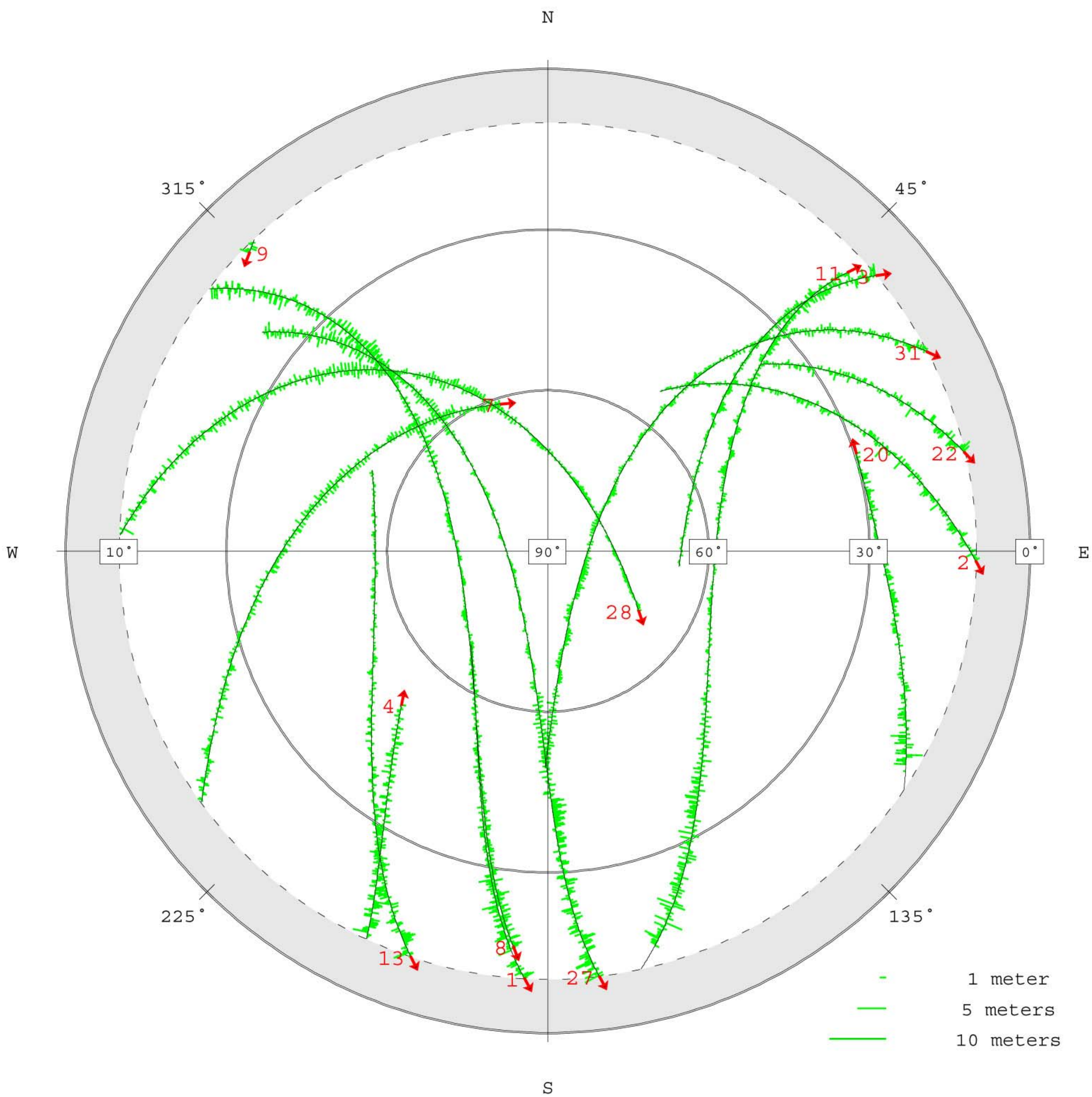

Figure 20. C1 Pseudorange Multipath at OKEE

Lat: 42.9139° Lon: -82.5949° Ell Ht: 160.8 (m)

GPS Time: Start 2002/08/28 00:00:00 Stop 2002/08/28 06:00:00

Figure 21. P2 Pseudorange Multipath at OKEE

Lat: 42.9139˚ Lon: -82.5949˚ Ell Ht: 160.8 (m)

GPS Time: Start 2002/08/28 00:00:00 Stop 2002/08/28 06:00:00

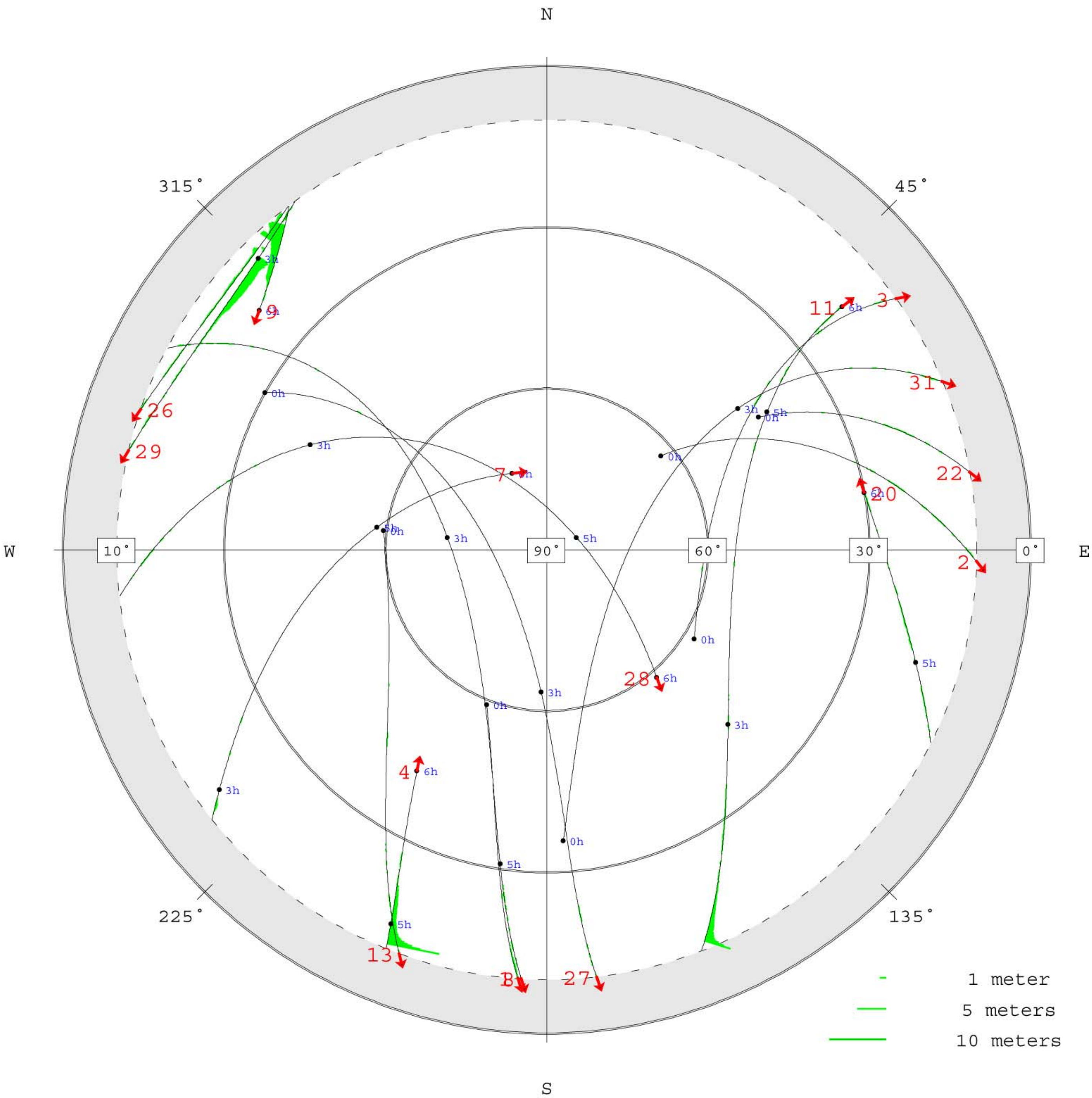

Figure 22(a). MP1 vs MP2 for 12 Different Receiver/Antenna Combinations

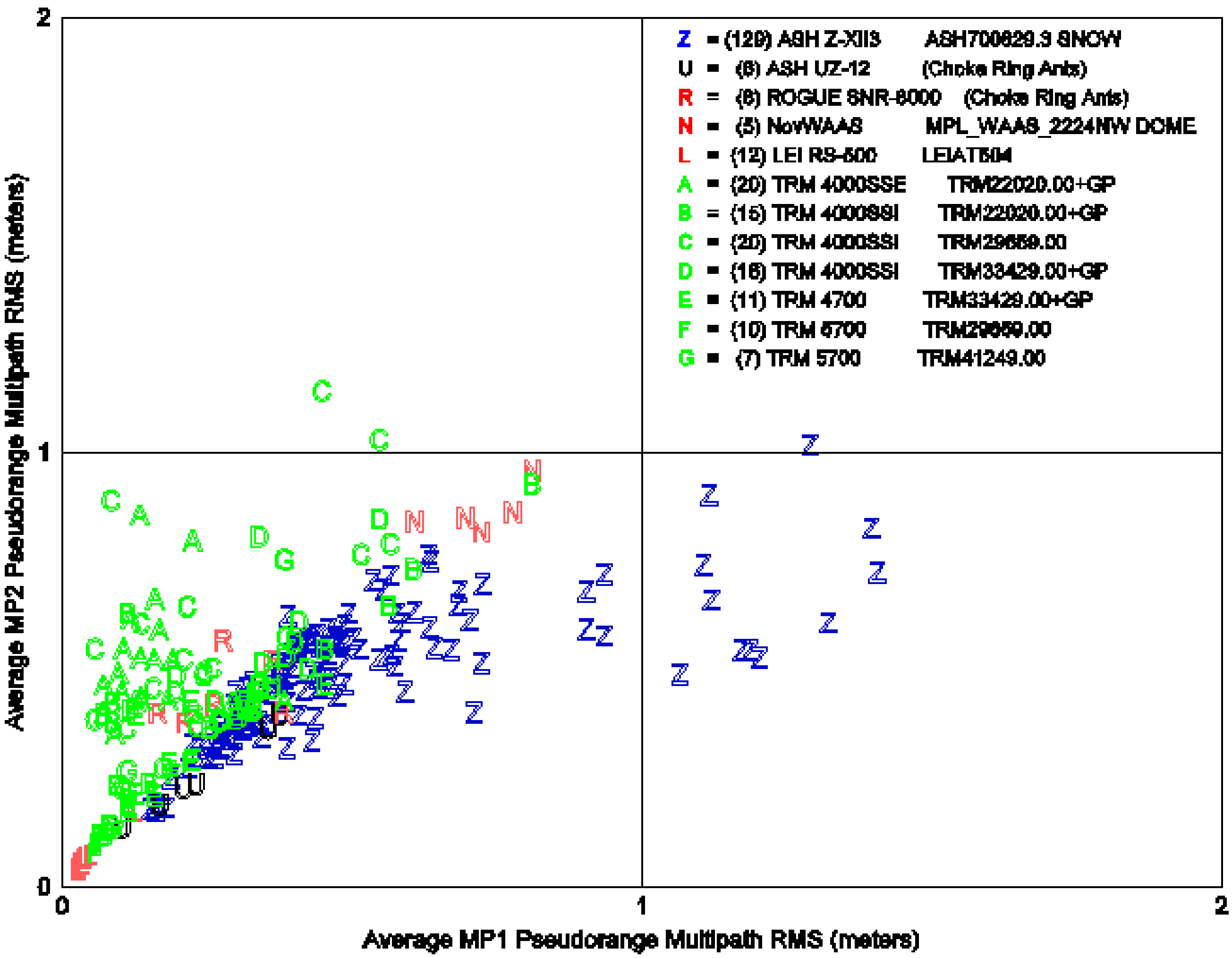

Figure 22(b). MP1 vs MP2 [Enlarged to show detail]

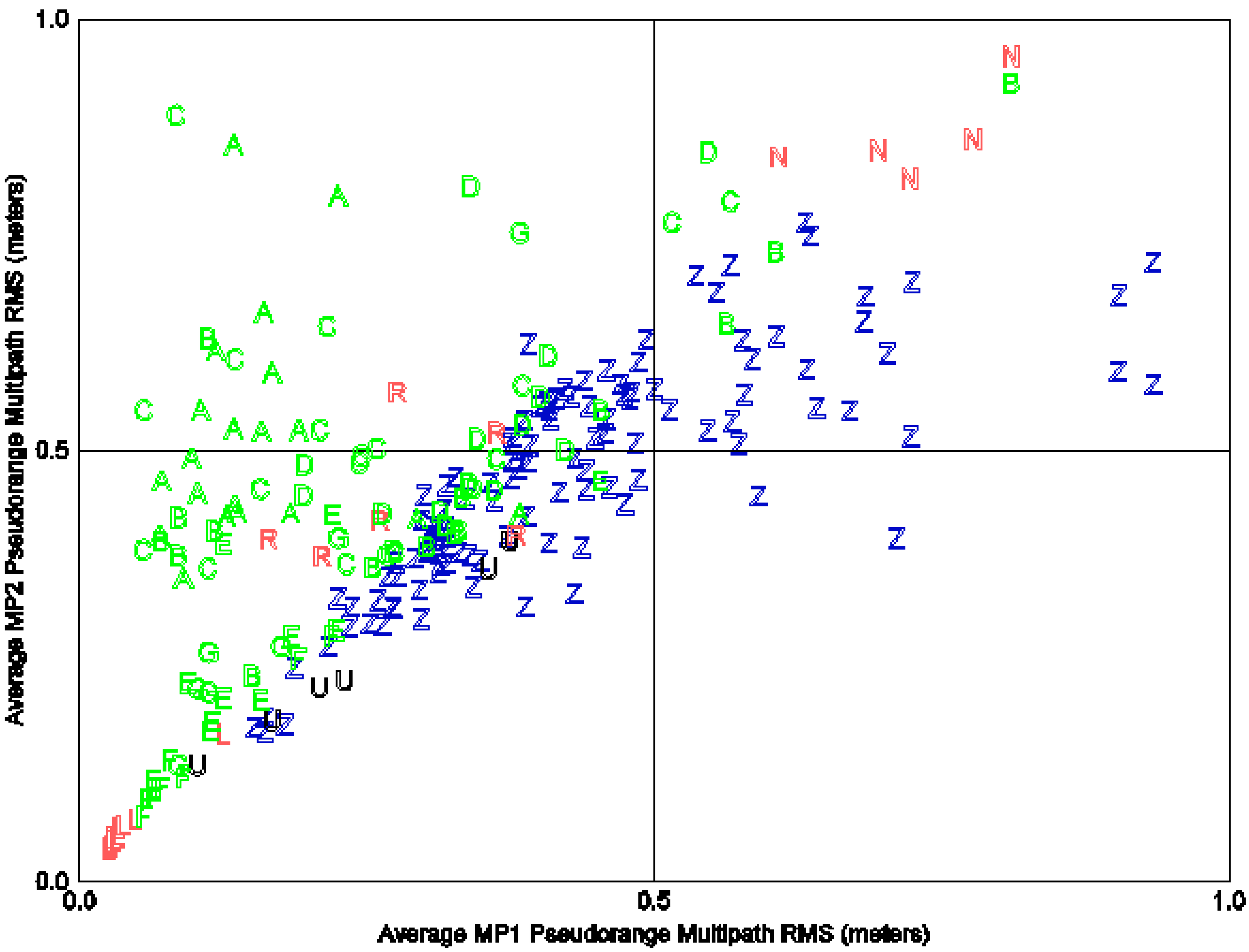

Table 1. Average MP1 RMS (40 Best stations listed highest to lowest) 20 Elev. Cutoff

Rank	MP1	StdDev	Site	#Days	Receiver Type	Antenna Type		Firmware Version
362	0.0859	0.0207	will	113	TRIMBLE 4000SSI	TRM22020.00+GP		7.29
363	0.0855	0.0279	pit1	109	TRIMBLE 4000SSI	TRM22020.00+GP		7.29
364	0.0853	0.0164	bsmk	43	TRIMBLE 5700	TRM41249.00		1.04
365	0.0813	0.0140	fdtc	106	TRIMBLE 4000SSI	TRM29659.00		7.32
366	0.0795	0.0069	bsmk	20	TRIMBLE 5700	TRM33429.00+GP		1.04
367	0.0787	0.0043	ospa	30	TRIMBLE 5700	ASH701945B_M		1.04
368	0.0781	0.0384	pktn	73	TRIMBLE 5700	TRM29659.00		1.04
369	0.0718	0.0549	mcon	74	TRIMBLE 5700	TRM29659.00		1.04
370	0.0711	0.0092	corc	87	TRIMBLE 4000SSE	TRM22020.00+GP		7.29
371	0.0700	0.0153	stpl	18	TRIMBLE 4000SSI	TRM22020.00+GP		7.29
372	0.0697	0.0281	arl5	92	TRIMBLE 4000SSE	TRM22020.00+GP		7.29
373	0.0660	0.0500	sidn	72	TRIMBLE 5700	TRM29659.00		1.04
374	0.0650	0.0173	eprt	113	TRIMBLE 4000SSI	TRM29659.00	DOME	7.27
375	0.0649	0.0417	corb	104	TRIMBLE 4000SSI	AOAD/M_T		7.29
376	0.0642	0.0072	mins	90	ASHTECH Z-XII3	AOAD/M_T		1E95
377	0.0636	0.0171	gust	56	TRIMBLE 5700	TRM29659.00		1.04
378	0.0632	0.0063	puc1	110	TRIMBLE 4700	TRM33429.20+GP		1.30
379	0.0627	0.0459	colb	60	TRIMBLE 5700	TRM29659.00		1.04
380	0.0601	0.0159	npri	107	TRIMBLE 4000SSI	TRM29659.00	DOME	7.29
381	0.0583	0.0077	freo	71	TRIMBLE 5700	TRM29659.00		1.04
382	0.0559	0.0202	leba	74	TRIMBLE 5700	TRM29659.00		1.04
383	0.0556	0.0053	adks	9	TRIMBLE 4000SSI	TRM29659.00		7.22
384	0.0550	0.0055	adks	6	TRIMBLE 4000SSI	TRM29659.00	TCWD	7.22
385	0.0547	0.0290	s300	109	TRIMBLE 4000SSI	TRM29659.00		7.29
386	0.0478	0.0238	nor2	58	LEICA RS500	LEIAT504	LEIS	3.00
387	0.0425	0.0158	adri	60	LEICA RS500	LEIAT504	LEIS	3.00
388	0.0368	0.0095	sup1	57	LEICA RS500	LEIAT504	LEIS	3.00
389	0.0354	0.0095	siby	26	LEICA RS500	LEIAT504	LEIS	3.00
390	0.0335	0.0094	grar	68	LEICA RS500	LEIAT504	LEIS	3.00
391	0.0331	0.0176	brig	77	LEICA RS500	LEIAT504	LEIS	3.00
392	0.0313	0.0141	sup2	54	LEICA RS500	LEIAT504	LEIS	3.00
393	0.0290	0.0071	sowr	59	LEICA RS500	LEIAT504	LEIS	3.00
394	0.0287	0.0079	mple	52	LEICA RS500	LEIAT504	LEIS	3.00
395	0.0287	0.0183	univ	54	LEICA RS500	LEIAT504	LEIS	3.00
396	0.0260	0.0193	metr	68	LEICA RS500	LEIAT504	LEIS	3.00
397	0.0250	0.0152	nor1	66	LEICA RS500	LEIAT504	LEIS	3.00
398	0.0247	0.0148	bayr	75	LEICA RS500	LEIAT504	LEIS	3.00
399	0.0247	0.0161	sup3	53	LEICA RS500	LEIAT504	LEIS	3.00
400	0.0233	0.0058	okee	21	LEICA RS500	LEIAT504	LEIS	3.00
401	0.0233	0.0074	lans	39	LEICA RS500	LEIAT504	LEIS	3.00

Table 2. Average MP2 RMS (40 Best stations listed highest to lowest) 20 Elev. Cutoff

Rank	MP2	StdDev	Site	#Days	Receiver Type	Antenna Type		Firmware Version
362	0.1686	0.0648	nor3	59	LEICA RS500	LEIAT504	LEIS	3.00
363	0.1655	0.0359	elen	77	TRIMBLE 4000SSE	TRM29659.00	UNAV	7.29
364	0.1625	0.0095	chab	115	ASHTECH Z-XII3	ASH700936A_M		CB001D02
365	0.1624	0.0116	cndr	80	ASHTECH Z-XII3	ASH700936D_M		CB00 & 1D02
366	0.1516	0.0064	amc2	96	AOA SNR-12 ACT	AOAD/M_T		3.3.32.4
367	0.1508	0.0184	fair	92	AOA SNR-8100 ACT	JPL D/M+CRT		3.3.32.2 soc2rnx
368	0.1494	0.1119	cnmi	110	TRIMBLE 4700	TRM33429.20+GP	DOME	7.29
369	0.1471	0.0049	atl1	7	LEICA SR9500	LEIAT303		
370	0.1384	0.0487	pktn	73	TRIMBLE 5700	TRM29659.00		
371	0.1379	0.0077	uiuc	34	TRIMBLE 4700	TRM33429.00+GP		
372	0.1323	0.0180	bsmk	43	TRIMBLE 5700	TRM41249.00		1.04
373	0.1322	0.0283	jama	79	ASHTECH UZ-12	AOAD/M_TA_NGS		UG00
374	0.1210	0.0091	bsmk	20	TRIMBLE 5700	TRM33429.00+GP		1.04
375	0.1174	0.0558	woos	72	TRIMBLE 5700	TRM29659.00		1.04
376	0.1151	0.0067	puc1	110	TRIMBLE 4700	TRM33429.20+GP		1.30
377	0.1130	0.0053	ospa	30	TRIMBLE 5700	ASH701945B_M		1.04
378	0.1068	0.0618	mcon	74	TRIMBLE 5700	TRM29659.00		1.04
379	0.1058	0.0612	sidn	72	TRIMBLE 5700	TRM29659.00		1.04
380	0.0940	0.0643	colb	60	TRIMBLE 5700	TRM29659.00		1.04
381	0.0936	0.0208	gust	56	TRIMBLE 5700	TRM29659.00		1.04
382	0.0920	0.0104	freo	71	TRIMBLE 5700	TRM29659.00		1.04
383	0.0850	0.0113	mins	90	ASHTECH Z-XII3	AOAD/M_T		1E95
384	0.0781	0.0133	siby	26	LEICA RS500	LEIAT504	LEIS	3.00
385	0.0750	0.0194	adri	60	LEICA RS500	LEIAT504	LEIS	3.00
386	0.0745	0.0164	tsea	67	LEICA CRS1000	LEIAT504		5.16
387	0.0730	0.0251	leba	74	TRIMBLE 5700	TRM29659.00		1.04
388	0.0688	0.0287	nor2	58	LEICA RS500	LEIAT504	LEIS	3.00
389	0.0632	0.0104	sup1	57	LEICA RS500	LEIAT504	LEIS	3.00
390	0.0600	0.0236	brig	77	LEICA RS500	LEIAT504	LEIS	3.00
391	0.0573	0.0105	mple	52	LEICA RS500	LEIAT504	LEIS	3.00
392	0.0493	0.0108	sowr	59	LEICA RS500	LEIAT504	LEIS	3.00
393	0.0491	0.0136	sup2	54	LEICA RS500	LEIAT504	LEIS	3.00
394	0.0490	0.0098	grar	68	LEICA RS500	LEIAT504	LEIS	3.00
395	0.0446	0.0206	univ	54	LEICA RS500	LEIAT504	LEIS	3.00
396	0.0381	0.0235	metr	68	LEICA RS500	LEIAT504	LEIS	3.00
397	0.0368	0.0121	sup3	53	LEICA RS500	LEIAT504	LEIS	3.00
398	0.0365	0.0176	nor1	66	LEICA RS500	LEIAT504	LEIS	3.00
399	0.0356	0.0099	lans	39	LEICA RS500	LEIAT504	LEIS	3.00
400	0.0345	0.0172	bayr	75	LEICA RS500	LEIAT504	LEIS	3.00
401	0.0338	0.0080	okee	21	LEICA RS500	LEIAT504	LEIS	3.00

Figure 23. The METR site in the Michigan network

Figure 24. The COLB site in the Ohio network

References

Bishop, G.J., D.S. Coco, P.H. Kappler, and E.A. Holland (1994). Studies and Performance of a New Technique for Mitigation of Pseudorange Multipath Effects in GPS Ground Stations. In: *Proceedings of The Institute of Navigation's National Technical Meeting*, San Diego, California, January, pp. 231-242.

Brown, A., and J. Wang (1999). High Accuracy Kinematic GPS Performance using a Digital Beam-Steering Array. In: *Proceedings of ION GPS-99*, Nashville, Tennessee, September 14-17, pp. 1685-1693.

Estey, L.H., and C.M. Meertens (1999). TEQC: The Multi-purpose Toolkit for GPS/GLONASS Data. *GPS Solutions*, Vol. 3, No. 1, pp. 42-49.

Kee, C., and B. Parkinson (1994). Calibration of Multipath Errors on GPS Pseudorange Measurements. In: *Proceedings of ION GPS-94*, Salt Lake City, Utah, September 20-23, pp. 353-362.

Ray, J.K. (1999). Use of Multiple Antennas to Mitigate Carrier Phase Multipath in Reference Stations. In: *Proceedings of ION-99,* Nashville, Tennessee, September 14-17, pp. 269-279.

Wanninger, L., and M. May (2001). Carrier-Phase Multipath Calibration of GPS Reference Stations. *Journal of The Institue of Navigation*, Vol. 48, No. 2, pp. 113-124.

Wolfe, D.B., C.L. Judy, E.J. Haukkala, D.J. Godfrey (2000). Implementing and Engineering an NDGPS Network in the United States. In: *Proceedings of ION 2000*, Salt Lake City, Utah, September 19-22, pp. 1254-1263.

Acknowledgements

The photographs for stations CHA1, CHA2, and FDTC in South Carolina were supplied by Lewis Lapine and Dick Woods of the South Carolina Geodetic Survey. The photographs for stations LOU1 and LOU2 in Kentucky were supplied by Ross MacKay, the NGS State Advisor for Kentucky. The photographs for stations YOU1 and YOU2 in New York were supplied by David Conner, the NGS State Advisor for Ohio. The photographs for stations RED1 and RED2 in Delaware were supplied by Mr. Ed Berchtold. The photographs of stations RIS1 and RIS2 in Iowa were supplied by Mr. Charles Smith of the U.S. Coast Guard. All other photographs of individual sites were taken from the NGS CORS website: http://www.ngs.noaa.gov/CORS .

Product Disclaimer

Mention of a commercial company or product does not constitute an endorsement by the National Oceanic and Atmospheric Administration. Use for publicity or advertisement purposes of information from this paper concerning proprietary products or the comparison of such products is not authorized.